



Effect of particle size distribution on the properties of celsian based glazes

Betül Yıldız¹

Received: 29 January 2024 / Revised: 29 April 2024 / Accepted: 9 June 2024
© The Author(s) 2024

Abstract

The microstructure and surface properties of ceramic glaze are influenced by chemical composition, particle size distribution, glaze application conditions, and firing parameters. This study specifically focused on the influence of glaze particle size distribution on the thermal behavior, microstructure, and surface appearance of barium frit based ceramic glaze in the floor tile firing process. The investigation involved examining the impact of four distinct particle size dimensions (d_{50} : 5.7 μm , 6.8 μm , 7.5 μm , 10.9 μm) on the glaze properties by using hot stage microscopy, X-ray diffraction (XRD), scanning electron microscopy (SEM), color and gloss measurements. The studies indicated that celsian is the dominant phase in the glaze structure. The sintering and softening temperatures of glazes decreased with the increase of milling time. A decrease in the particle size of the glaze slurry increased the whiteness index. As the average particle size (d_{50}) of the glaze decreased, the number of crystals was also increased. The investigation results also suggested a relation between specular reflection and milling time. As the milling time extended, there was a corresponding increase in the magnitude of glossiness.

Keywords Glaze · Particle size distribution · Surface appearance of glaze · Ceramic tile · Industrial firing

Introduction

Ceramic glaze comprises carefully chosen raw materials. After grinding and applying to a ceramic body, it undergoes a firing process, resulting in transformation into a vitrified coating, whether in whole or part. Glaze imparts chemical neutrality, impermeability to liquids and gases, ease of cleaning, a smooth surface, and resilience against abrasion, scratches, and mechanical stress [1, 2].

In addition to its functional attributes, the glaze plays a crucial role in the aesthetic appeal of the ceramic tile. The aesthetic features encompass a wide range of surface finishes, including varying degrees of gloss and matte, color differences, and distinctive surface appearances [3]. The integration of both aspects is vital from a commercial perspective, primarily related to the surface properties of the glazes [1, 4]. The glaze compositions used for producing

matt glazes in tile manufacturing are generally made up of frits and other raw materials, so that the glazes' appearance could be due to the presence of crystals. The crystals found in a matt glaze may come from (a) the addition of raw materials to the glaze composition, which remains undissolved in the glassy phase formed during firing, (b) crystallisation, during firing of the glaze composition of crystalline phases from the glassy matrix that forms during firing [5]. Common variations include lime matte with wollastonite (CaSiO_3) crystals and zinc matte with willemite (Zn_2SiO_4) crystals [6]. In addition to wollastonite and willemite-based glaze, so-called barium matts in producing matt glaze surfaces have spread in glazed ceramic tile production. These glazes comprise frits with a high BaO content, which, according to the literature surveyed, give rise to celsian crystallisation ($\text{BaAl}_2\text{Si}_2\text{O}_8$) [5].

Matt glazes present a higher surface roughness than that found in glossy glazes. This surface roughness causes multiple reflections of incident light, reducing the amount of light reflected in the specular direction and, therefore, producing a loss of gloss. The quantity of light reflected depends not only on the surface roughness but also on the refractive index of the material and the angle of incident light. Typically, the

✉ Betül Yıldız
betul.yildiz@bilecik.edu.tr

¹ Department of Metallurgy and Materials Engineering,
Bilecik Şeyh Edebali University, Bilecik 11100, Turkey

surface roughness of matte glazes results from including crystals. However, whether this roughness is due to crystals near or on the surface or an increase in glaze viscosity in the molten state remains unverified. The presence of these crystals is believed to impede optimal surface stretching. It should be taken into account that any glaze with very high viscosity, even without crystals, yields a matt surface since it impedes adequate smoothness of the surface [5, 7].

Typically, the microstructure of glaze consists of a predominant amorphous phase, enclosed bubbles, and a minimal proportion of crystalline phase [8]. The changes in microstructure in matte glazes impact both aesthetic and functional properties. The microstructure development is influenced by the chemical composition, particle size distribution of the glaze, and the conditions of glaze application and firing parameters.

When the literature studies examining the effect of glaze particle size distribution (PSD) on the glaze are generally evaluated, it is observed that the relevant studies can be categorized into research on the impact of PSD on its thermal properties [9, 10], studies on its influence on the microstructure [11–13], studies on its effect on the optical properties of the glaze [4, 14, 15], and studies on its effect on the functional properties of the glaze [16, 17].

Natalia et al. investigated the effect of PSD of two types of single-firing transparent lead glazes commercial glazes on the glaze melting behavior. They used differential thermal and thermogravimetric analysis and hot-stage microscopy to examine the relationship between particle size and the thermal behavior of the glaze. They didn't reported any data about surface appearance and microstructure in their study [9].

Jiyuan et al. investigated the PSD of sanitaryware glaze on the surface appearance of glaze. Thermal behavior of the glazes with different particle sizes (from 2.14 to 2.78 μm .) was investigated by a hot stage microscope. The study did not report color indices, glossiness, and microstructure analyses [10].

Wattanasiriwech et al. investigated the impact of glaze powder particle size and glaze layer thickness on a dolomite body. They applied a fritted glaze with five different average particle sizes to a pre-fired body, which was then glaze-fired at 1000 °C for 60 min in an electric furnace. Their investigations unveiled that when the average particle size of the glaze powder was around 1 micron or smaller, the glaze coating displayed a proclivity to develop cracks and eventually manifested cloudiness, attributed to the abundance of bubbles within the glaze layer [11]. In the study, color measurements and microstructure analyses were not reported.

Amaros et al. investigated the sinter-crystallization kinetics of a glaze within the $\text{SiO}_2\text{-Al}_2\text{O}_3\text{-CaO-MgO-SrO}$ system, leading to the devitrification of anorthoclase and

diopside. The study involved three different particle size distributions for the glazes, with average particle size distributions of 9.6 μm , 4.0 μm , and 0.65 μm . Their findings indicated that as the average particle size (d_{50}) of the glaze decreased, there was an observed increase in the number of crystals, accompanied by a reduction in the size. However, they didn't examine the thermal behavior and the optical characteristics of glaze and used a laboratory kiln in their study [12].

Amoros et al. explored how the distribution of particle sizes influences the formation of the glaze microstructure and firing shrinkage across different firing temperatures. Their study employed a thermal treatment approach, involving heating at a 15 K/min rate to reach the firing temperature, conducted in a laboratory kiln [13]. They didn't report glaze optical characteristics in the study.

Felisbino et al. also studied the particle size dimension effect of matte glaze on the glossiness of the glaze. The study findings indicated a direct proportionality between specular reflection and milling time; therefore, as the glaze milling time increased, there was a corresponding increase in the magnitude of glossiness. In the study, thermal analyses, color measurements, and microstructure analysis were not reported [14].

Bernardin investigated the influence of PSD on the surface appearance of glazed tiles. It was demonstrated that decreasing the glaze particle size has reduced molten glaze viscosity, which caused uniformity in the glass layer and produced a glaze with a smooth surface [15]. In the study laboratory type kiln was used for the experiment. The study did not report the influence of particle size distribution on the thermal behavior of glaze and microstructure evolution.

Partyka and Lis studied the effect of the particle size distribution of raw materials on the optical properties of sanitary glaze compositions. The samples were prepared in laboratory and they grouped the raw materials in three category; -quartz based, feldspar based, and others. They noticed that the preparation of glazes by using controlled grain size raw materials can advantageously influence the surface properties of ceramic glazes. Decreasing the grain size of zirconium silicate can notably improve glaze whiteness and glossiness, albeit with a potentially adverse effect on roughness. It was advised to independently optimize the grain sizes of quartz and feldspar to attain the most favorable surface features in the glaze [4].

Previous studies in the literature have highlighted the significance of particle size distribution (PSD) as a crucial factor in determining glaze properties. Nevertheless, these experiments predominantly involved laboratory firing conditions and did not involve a holistic approach. To fill this gap in the literature, this study aimed to determine a relationship between particle size distribution, thermal behavior,

Table 1 Particle size distributions of glaze suspensions

| Glaze Code | Milling time (minutes) | d (0.1) | d (0.5) | d (0.9) |
|------------|------------------------|---------|---------|---------|
| D2 | 20 | 1.800 | 10.906 | 37.116 |
| D3 | 30 | 1.447 | 7.571 | 28.972 |
| D4 | 40 | 1.553 | 6.862 | 26.761 |
| D5 | 50 | 1.382 | 5.761 | 22.111 |

microstructure, and optical properties in the glazes prepared with barium-based frits. The investigation was carried out under the industrial porcelain tile firing regime.

Experimental methods

Ceramic glaze preparation

This study involved a glaze formulation that incorporated 8% kaolin by weight and standard additives into a commercial frit composition rooted in a SiO₂-Al₂O₃-CaO-BaO-ZnO system.

Aqueous suspensions of the mentioned glaze, incorporating 0.2% sodium carboxymethylcellulose and 0.2% sodium tripolyphosphate by weight, with a solids volume fraction of 0.70, underwent wet milling in a laboratory mill to yield distinct glaze particle size distributions. In the study, different milling durations therefore different particle size dimensions, were determined by considering the glaze milling durations and sieve residues commonly used in the ceramic tile industry and the studies in the literature. When evaluating studies concerning the effect of particle size on the ceramic glaze surface, it has been observed that the grinding durations in these studies range from 5 to 60 min [9, 10, 14, 15, 17] and d50 of the glazes varies in a wide range from 11.20 to 0.65 μm [9, 10, 12, 13, 15, 17]. Within this context, the current study also considered this range in the literature, incrementally increasing the duration from 20 min with intervals of 10 min, up to 50 min. The particle size distributions of the glaze after the milling stage were analysed using a laser diffractometer with a resolution of 0.5 μm, and the results are provided in Table 1. Varying the milling time from 20 to 50 min yields d50 values for D2–D5 that range from 10.906 μm to 5.761 μm. The milling time utilized in the study and the obtained average particle size values (d50) are also consistent with the study conducted by Taşkıran et al. [17], which investigated the effect of particle size distribution on the optical and chemical resistance of floor tile glazes.

The chemical composition range of the frit composition is given in Table 2. The recipes worked in the study were named based on grinding time. Recipes grind for 20, 30, 40 and 50 min were respectively labeled as D2, D3, D4 and D5 glazes.

The glaze slurries formulated exhibited a measured density ranging from 1.80 to 1.81 g/cm³ and fluidity corresponding to an outflow time from a 4 mm Ford Cup equivalent to 18–20 s. The prepared aqueous glaze suspensions were applied to commercial raw porcelain tile bodies using a 0.8 mm glaze applicator. The glazed porcelain bodies were dried at 110 °C for 30 min. The glazed porcelain tile samples were then fired in an industrial fast-fired gas kiln at a temperature of 1210 °C for a total duration of 39 min.

Characterization of fired glazed samples

The color parameters L*, a*, and b* and the samples' glossiness (measured at an angle of 80 °) were determined by using a Minolta CR-300 series chromometer. To ensure the accuracy of the results, color and glossiness measurements were repeated three times for each sample, and the average of the obtained data was calculated.

The thermal behavior of the samples was examined using a heating microscope (Misura 3 HSM Hot-stage microscopy, Expert Systems, Srl, Modena, Italy). Glaze powders were prepared through uniaxial dry pressing in a cylindrical mold (2 mm x 3 mm) and then subjected to heating, with a temperature ramp from room temperature to 1300 °C at a rate of 10 °C per minute. The characteristic temperatures of the samples were determined through automatic software analysis (Misura 3.32), which calculated geometric parameters based on the sample's shape.

X-ray diffraction analysis (XRD) was conducted using a Rigaku Miniflex 600 diffractometer at 40 kV and 15 mA. Glazed samples were scanned in the range of 2θ, 20–80 °. The microstructure of the glazed tiles was investigated using scanning electron microscopy (Hitachi Regulus 8230 with EDS).

Results and discussion

Thermal characterization of glazes

In glazes, densification is achieved through sintering in the presence of a viscous flow at temperatures slightly above the glass transition temperature (T_g), forming a densely

Table 2 Chemical composition of the frit

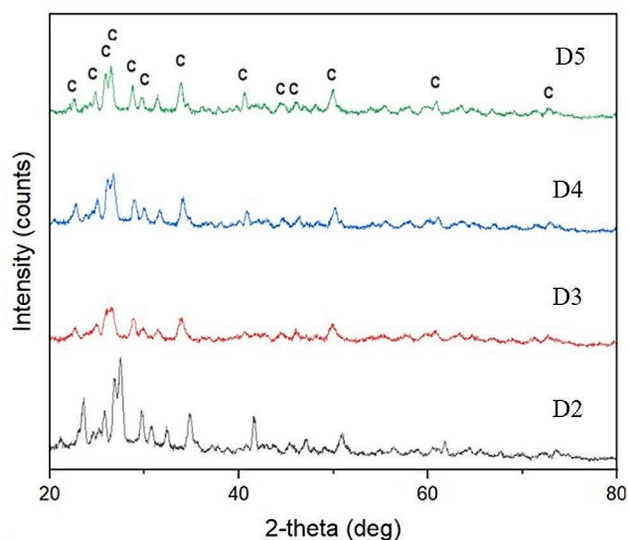
| Oxide Wt.% | Na ₂ O | K ₂ O | CaO | BaO | ZnO | Al ₂ O ₃ | B ₂ O ₃ | SiO ₂ |
|---------------|-------------------|------------------|------|------|------|--------------------------------|-------------------------------|------------------|
| Ba-based frit | 1–5 | 1–5 | 7–15 | 7–15 | 7–15 | 10–18 | 1–8 | 45–55 |

Table 3 Characteristic temperatures of glazes

| Temperature (°C) | D2 Glaze | D3 Glaze | D4 Glaze | D5 Glaze |
|------------------|----------|----------|----------|----------|
| Sintering T. | 868 | 848 | 852 | 834 |
| Softening T. | 872 | 850 | 854 | 836 |
| Sphere T. | - | - | - | - |
| Half Sphere T. | 1162 | 1156 | 1156 | 1156 |
| Fusion T. | 1166 | 1166 | 1162 | 1172 |

packed layer with minimal porosity [3]. The hot stage microscope plays a crucial role in this process. It provides valuable information such as the sintering of grains (starting from milled material), softening of the glaze sample, and the temperatures or intervals where these phenomena occur [18]. The sintering temperature, as determined by the hot stage microscope, is the temperature at which the sample exhibits a dimensional variation equivalent to 5% of the initial image acquired, considered as 100%. The softening point is achieved when liquid phases become apparent on the surface of the sample. Subsequently, notable changes in the sample's shape occur as a result of the surface tension exerted by the liquid phases. The sphere temperature is a significant stage in the glaze melting process. At this temperature, the sample predominantly consists of liquid phases, and the sample's shape is governed by surface tension. However, certain glasses characterized by high density and low surface tension may not attain the sphere point. The half sphere temperature is reached when the height of the sample is half the width of the base. When the sample's height decreases to less than one-third of the base, it is inferred that the sample has fully liquefied, indicating it has reached the melting point [19].

The effect of the glaze particle size on the thermal behavior of studied glazes is shown in Table 3. With the average particle size in the studied glazes decreasing from 10.906 to 5.761, the sintering and softening temperatures have respectively decreased from 868 °C to 834 °C and 872 °C to 836 °C. None of the studied glazes showed sphere temperature. No correlation has been reached between the particle size distribution of the glaze and the half sphere and fusion temperatures of the samples. It can be seen that the glaze sinterability increases with decreasing mean particle size. This result is consistent with the literature. Gorodlova et al. studied the impact of particle size reduction on glaze-melting behavior. The study used two types of commercial single-firing transparent lead glazes. They milled the glaze at different milling times (0 min., 5 min., 10 min., 20 min., and 60 min.), and they investigated the PSD effect on glaze melting behavior by using a hot stage microscope, optical dilatometer, and making differential and thermogravimetric analysis. Their results also indicated that glazes with lower mean size values began to sinter and deform at lower temperatures [9]. In another study, Li et al. examined the impact

**Fig. 1** XRD patterns of the studied ceramic glazes (C: Celsius)

of particle size distribution in raw glazes on the appearance of glazed surfaces. They subjected the raw glazes to milling in a ball mill for 15, 20, 30, and 40 min to achieve this. The resulting glaze slurries were applied to green bodies intended for sanitary wares. After application, dried samples underwent firing at 1220 °C in a laboratory electric furnace. The researchers analyzed the thermal behavior of the glazes using a hot-stage microscope and conducted differential and thermogravimetric analyses. Their observations revealed that smaller particle-sized glazes exhibited easier melting [10]. Taşkıran et al. explored the impact of glaze particle size distribution on the surface properties of floor tile glazes. They used a commercial matt frit and raw materials to produce matt glazes. Glaze compositions were milled with alumina balls for 10, 20, 30, and 40 min. After applying the glaze to the porcelain tile, the glazed tiles were fired in an industrial fast-firing regime. A hot-stage microscope investigated the thermal behavior of the glazes. They also indicated that glaze sinterability is increased with decreasing mean particle size from 11.2 µm to 7.26 µm [17]. The decrease in sintering and softening temperatures can be attributed to the increased contact points between particles trigger material transport and influence the viscous flow of glaze systems [9, 20, 21].

Microstructure and phase analysis

Figure 1 represents the crystalline phases after sintering the glazes through the different milling times. Celsius phase is the only phase detected in all samples. Altındel et al. explored the influence of variations in BaO-Al₂O₃ on BAS glass-ceramic glaze. They observed the initiation of Celsius crystallization at temperatures approximately between

800 and 820 °C and 909–918 °C [22]. In another study, Da Silva et al. recorded the crystallization of $\text{BaAl}_2\text{Si}_2\text{O}_8$ in BAS glass-ceramic over a temperature range of 870 °C to 1050 °C [23]. Therefore it can be stated that the maximum temperature in the study which is 1210 °C is enough for celsian crystallization.

The intensity of the peaks decreased with increasing milling time in XRD analysis (Fig. 1). This result is not consistent with the literature. Taşkıran et al. observed anorthite and free quartz peaks in their study. They reported that the peak intensity of the anorthite phase increased with increasing milling time and they explained this result with crystallization. They indicated that the crystallization is increased with decreased particle size for the same sintering regime and glaze composition [17].

Backscattered SEM images with low magnification (500X) of the glazes in Fig. 2 show higher crystallization in the glaze structure. With the increase of the milling time and thus lower particle size distribution, there is a notable rise in the amount of crystal phase within the glassy phase. This result is seen in the difference between D2 and D5 SEM images (Fig. 3). Bubbles are seen in all the glaze microstructures. In all ceramic glazes, air bubbles occupy specific volumetric fractions and exhibit diverse size distributions, dependent on the products' nature and the manufacturing conditions. These bubbles may arise from gases released by the support during firing, air trapped among frit particles in the green compact or the inclusion of air bubbles present in the suspensions utilized for wet glaze application [24].

Fig. 2 FESEM-BSE images of the cross-section of the studied ceramic glazes (magnification 500X); (a) D2, (b) D3, (c) D4, (d) D5

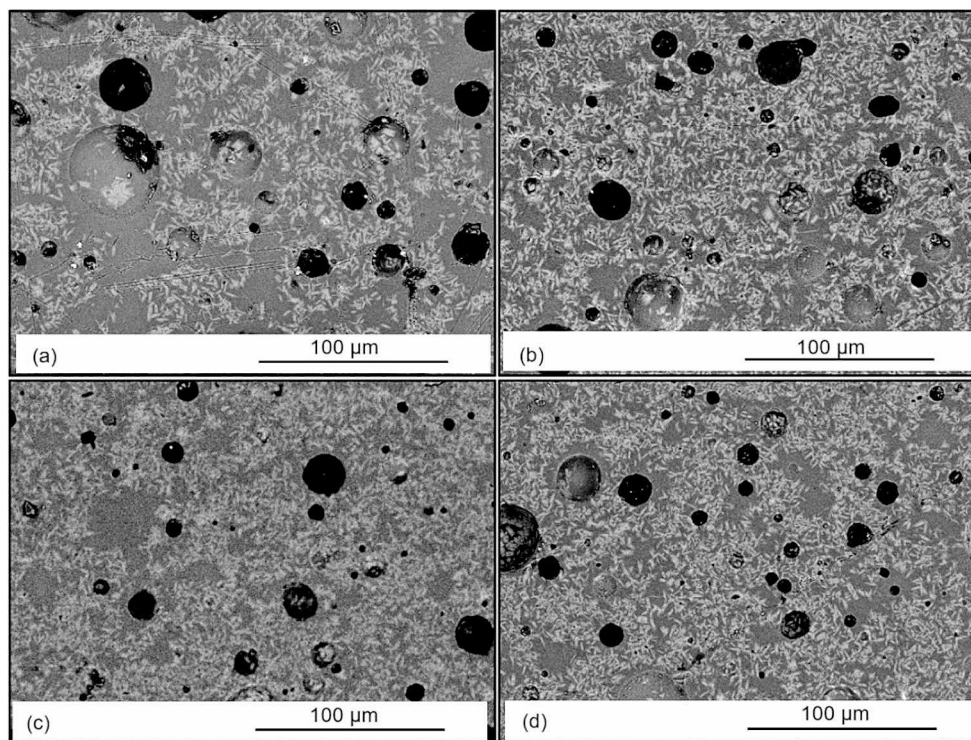


Figure 3 shows that the needle-like crystal size generally varies between 2 and 7 μm . Based on the grinding time, the SEM images indicate no noticeable change in crystal grain size and shape in the obtained glaze microstructures.

Figure 4 and Table 4 present the EDS patterns and element wt% measured in the matrix of glazes, whereas Fig. 5 and Table 5 depict those measured within the crystal phase of the glazes. The elements detected in the glassy phase are Na, K, Ca, Zn, Al, Si and O and the elements detected in the crystal phase are Na, K, Ba, Zn, Al and Si. A clear correlation emerges from the results - the Ba content in the matrix is crystallized as celsian crystals. This result aligns with the XRD analysis, clarifying the findings.

Optical properties

The critical optical features include the percentage of specular reflection, influencing brightness, and the quantity of transmitted light, determining color, depth, saturation, etc. These characteristics are contingent upon the fraction of diffusely transmitted light. The opacity and coverage properties of ceramic glazes hinge on the extent of diffuse light reflection from the top surface before reaching the bottom surface. In the case of translucent glasses, most light needs to be transmitted, with only a portion being diffusely reflected. The opacifying capability is thus reliant on light scattering induced by particles or nuclei within the binary system, directly linked to the secondary phase's size, shape, concentration, and refractive index [25]. Hence, for optimal

Fig. 3 FESEM-BSE images of the cross-section of the studied ceramic glazes (magnification 2500X): (a) D2, (b) D3, (c) D4, (d) D5

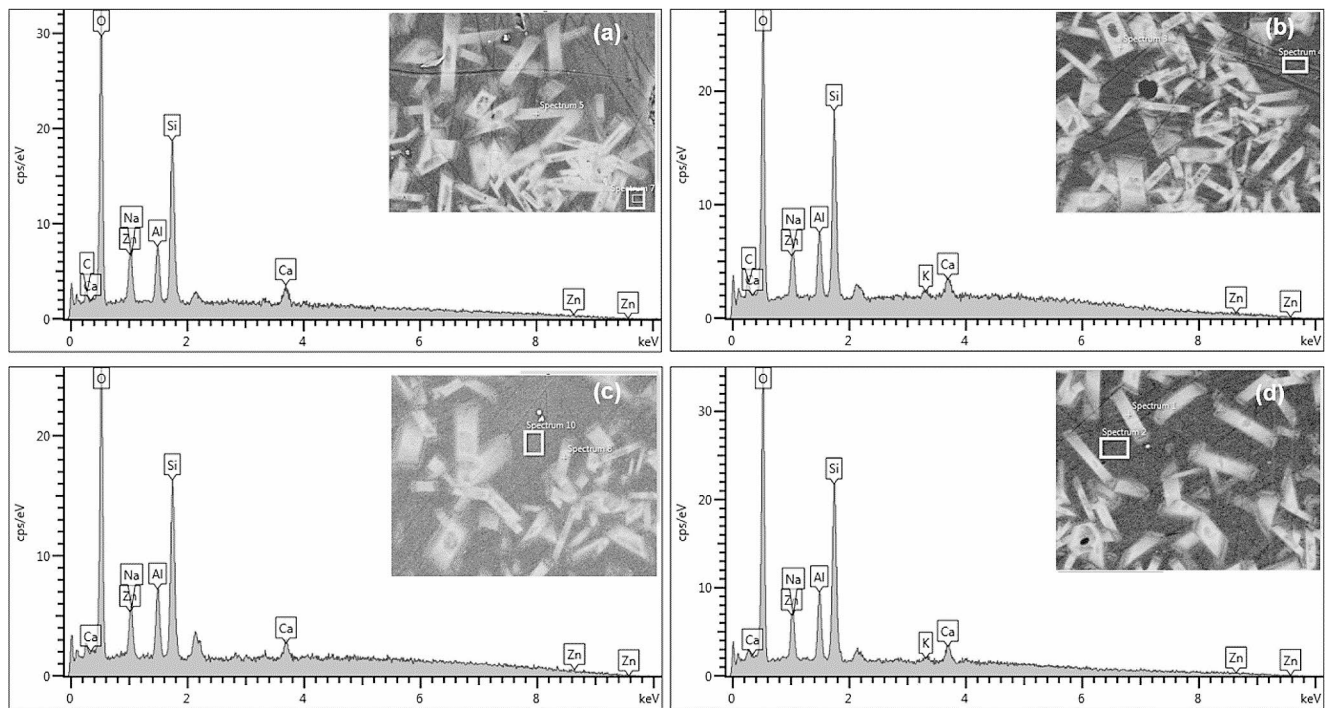
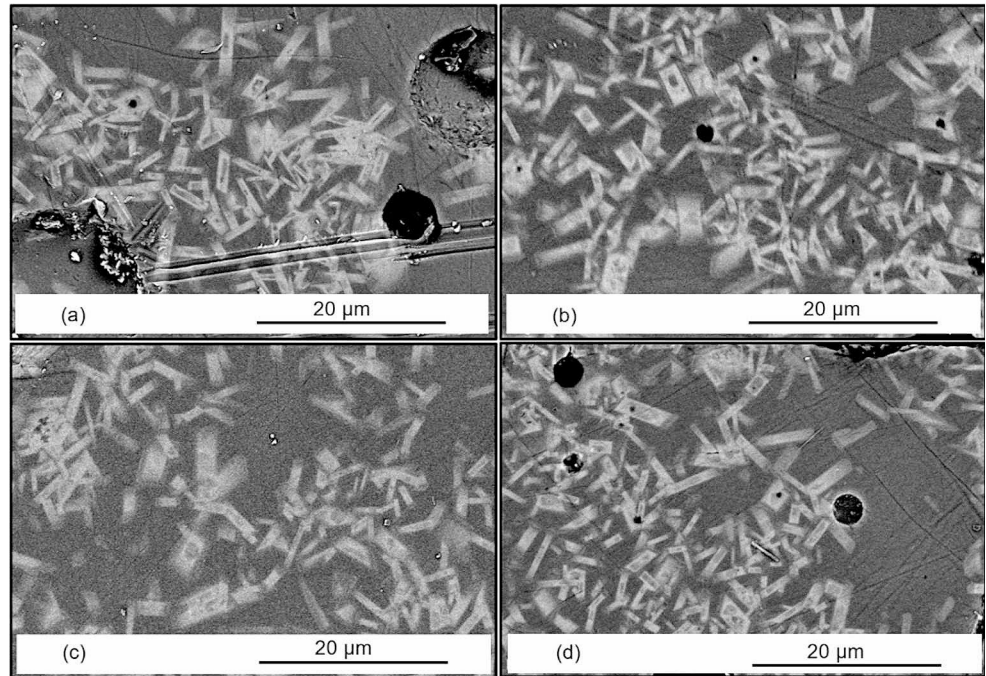


Fig. 4 EDS patterns of the glazes taken from the glassy phase; (a) D2, (b) D3, (c) D4, (d) D5

Table 4 Element wt%. measured in the cross-section of the glassy phase FESEM- EDX

| Glaze | O | Na | Al | Si | Ca | Zn | K |
|-------|-------|------|------|-------|------|------|------|
| D2 | 52.69 | 1.53 | 6.73 | 22.36 | 7.36 | 9.33 | - |
| D3 | 50.48 | 2.62 | 7.16 | 23.17 | 7.59 | 6.99 | 1.99 |
| D4 | 50.19 | 2.62 | 8 | 23.98 | 7.80 | 7.43 | - |
| D5 | 50.04 | 1.93 | 7.72 | 23.15 | 7.67 | 8.02 | 1.47 |

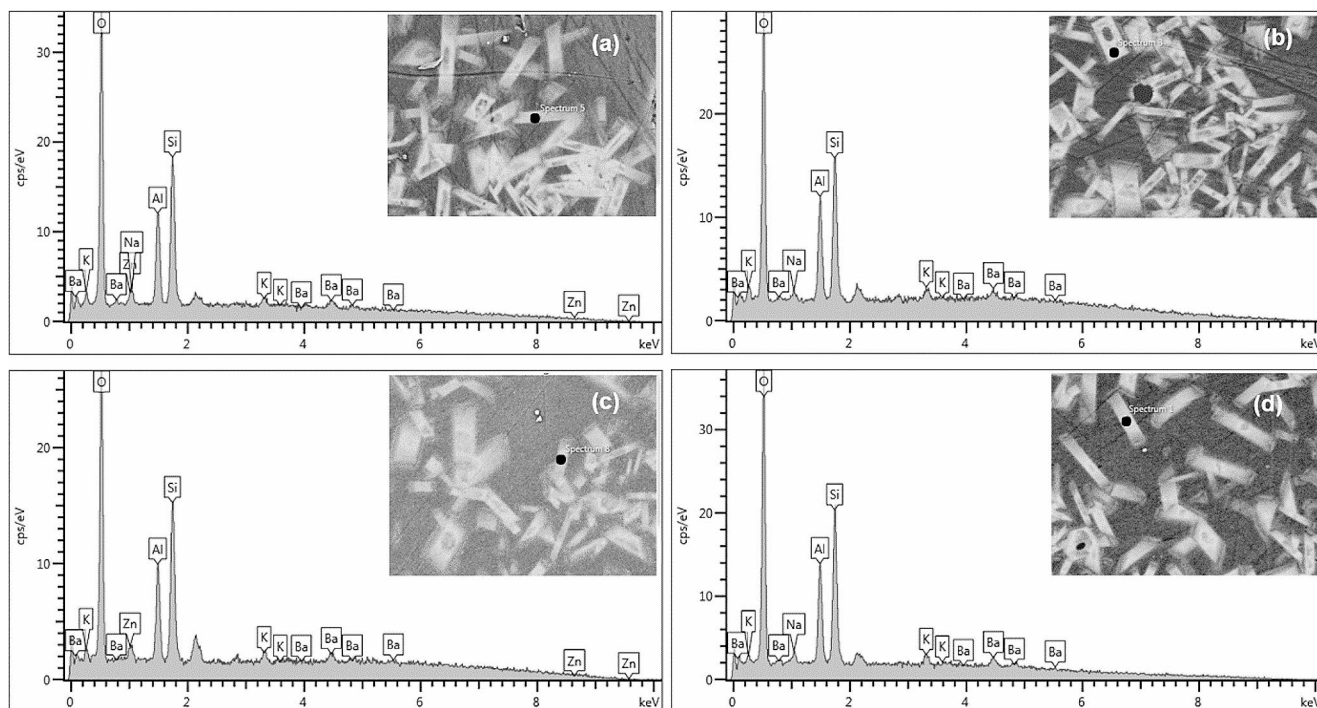


Fig. 5 EDS patterns of the glazes taken from the crystal phase; (a) D2, (b) D3, (c) D4, (d) D5

Table 5 Element wt%. measured in the cross-section of the crystal phase FESEM-EDX

| Glaze | O | Na | Al | Si | Ba | Zn | K |
|-------|-------|------|-------|--------|-------|------|------|
| D2 | 42.98 | 0.95 | 11.68 | 21.37 | 18.58 | 1.76 | 3.18 |
| D3 | 42.10 | 0.87 | 12.42 | 20.860 | 19.77 | - | 3.99 |
| D4 | 39.02 | - | 10.83 | 20.84 | 22.19 | 3.05 | 4.06 |
| D5 | 40.87 | 1.20 | 11.85 | 20.78 | 21.45 | - | 3.86 |

light scattering, or, in other words, to enhance diffuse reflection, secondary phase particles need a refractive index significantly different from the matrix and a particle size comparable to the wavelength of the incident light. Additionally, maintaining a relatively high concentration of the second phase is crucial to ensure a substantial number of points for diffuse reflectance [26].

The refractive index of most glazes and ceramic enamels within silicate and borosilicate systems typically falls between 1.48 and 1.65. Consequently, opacifying agents need to possess a considerably higher refractive index. Indeed, the higher the refractive index of the opacifying agent, the greater the whiteness of the glaze. An ideal opacifying agent should produce tiny particles in silica matrix liquids while remaining entirely inert to the glass phase. Chemically, these agents must exhibit high inertia and insolubility in the glass matrix at low temperatures, precipitate within the glass cooling range, and display high solubility in glass at melting temperatures. This results in the opacifying agents forming through the recrystallization of the liquid medium, generating tiny crystals and achieving high coverage. This mechanism creates various opaque glasses and

glazes, including white zirconium frits and titanium dioxide enamels utilized in glazing applications [26].

Color (L^* , a^* , b^*) and gloss (80°) values of the glazes and photos of the glazes are represented in Figs. 6 and 7, respectively. According to the CIELAB model, $L^* = 0$ represents black, $L^* = 100$ represents white, a^* is green-red at the horizontal axis, and b^* is yellow-blue at the vertical axis [1]. Figure 6 shows that glaze milling time increases glazes' L^* values, whereas a^* and b^* values are decreased. Photos of the glaze surfaces also show that the whiteness increase from sample D2 to sample D5. Higher L^* values of the glazes indicated an insignificant increase in whiteness with increased milling time. Because of the same crystal type and matrix obtained in the studied glazes, this result could be linked to the presence of a more significant amount of celsian crystals, which was confirmed by SEM observations (Fig. 3). The higher amount of crystals caused a high number of diffuse reflectance points, therefore, higher whiteness.

Results also show that with the increase in milling time, the glossiness of the glazes also increases. Glossiness is related to the amount of light reflected in the specular

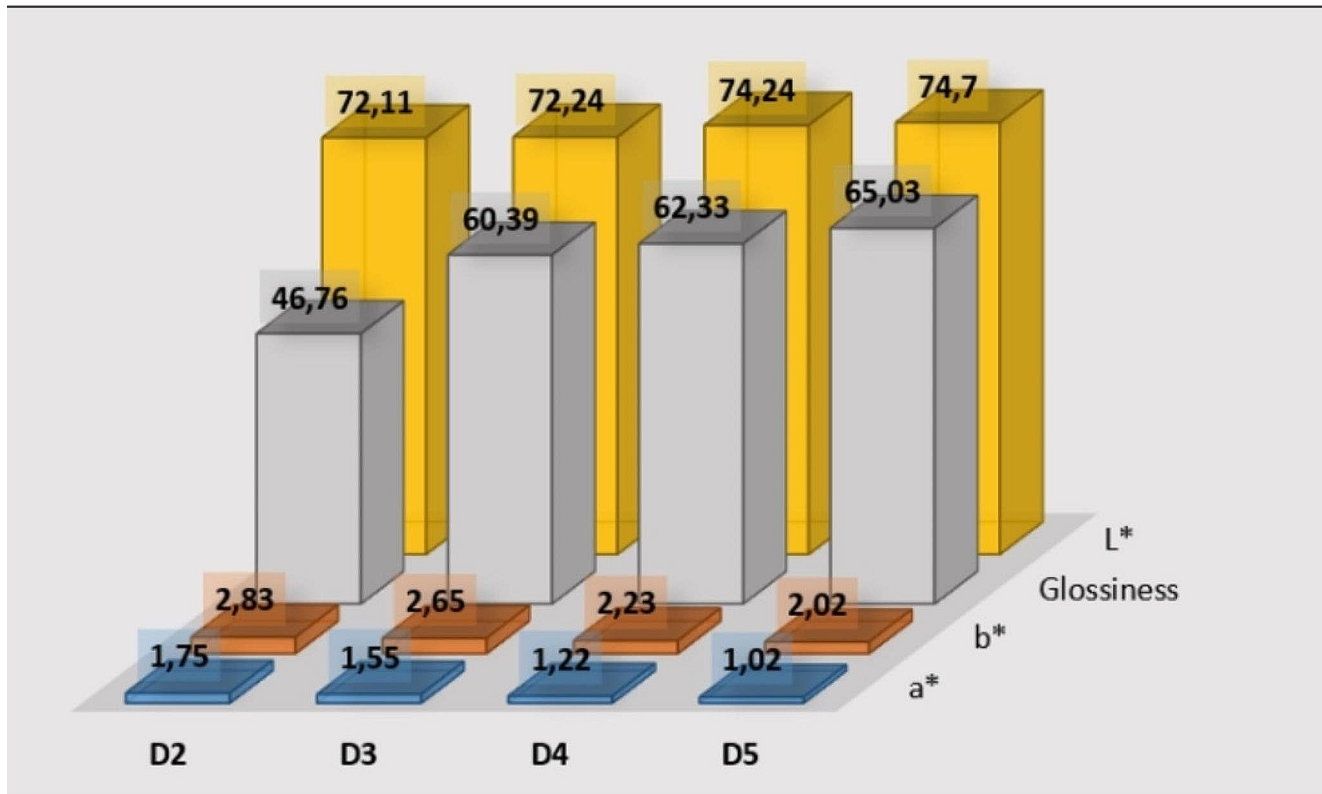


Fig. 6 Colour (L^* , a^* , b^*), gloss (80°) values of the glazes

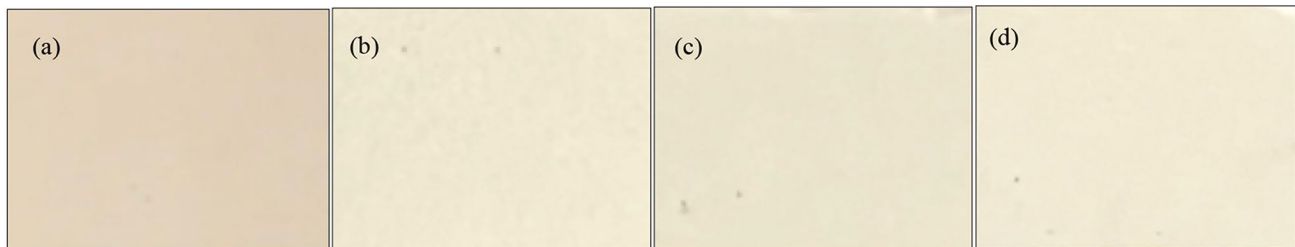


Fig. 7 Photos of the glaze surfaces: (a) D2, (b) D3, (c) D4, (d) D5

direction. The amount of reflected light is influenced not only by the surface roughness but also by the refractive index of the material and the angle of incident light [5]. For this study, the refractive index of the glaze can be assumed the same; therefore, the amount of reflected light and glossiness can be attributed to surface roughness. As a result of extended milling time, the particle size has reduced, causing an expansion in its surface area and consequently enlarging the contact region between particles. When applied to a ceramic surface, the glaze yielded a smoother appearance with minimal roughness, giving it a stretched appearance. The decrease in particle size gradually stretched the glaze surface, leading to an improved glaze reflection [15]. The results for particle size distribution and glossiness relation are consistent with the literature. Earlier research focused on

examining the influence of particle size distribution on the surface appearance of glazes. These studies demonstrated that an extended glaze milling time resulted in a heightened level of specular reflection, thereby enhancing glossiness [5, 14, 15].

Conclusions

In this study, it has been shown that the sintering and softening temperatures of the glazes prepared with barium-based frits decrease with milling time. It can be attributed to the higher surface energy of milled particles, which is responsible for an increased driving force in the sintering process. Additionally, a more significant number of contact points

between particles initiates material transport and affects the viscous flow of glaze systems.

The microstructure analysis showed that Celsian crystals are dispersed in the glassy matrix in the glazing structure. It was observed that regardless of the milling time, the needle-like Celsian crystals exhibited particle sizes varied between 2 and 7 microns. As the milling time increases, resulting in a finer particle size distribution, there is a noticeable increase in the quantity of crystal phase within the glassy phase.

Glaze whiter index (L^*) and gloss values increase with milling time. Due to the same crystal type and matrix acquired in the investigated glazes, higher L^* values may be attributed to the higher concentration of Celsian crystals, as verified through SEM observations. The increased abundance of crystals results in more diffuse reflectance points, leading to elevated whiteness. The increase in glossiness can be ascribed to the decrease in particle size, leading to a gradual stretching of the glaze surface and improved glaze reflection.

The results of this study would be helpful not only for floor tile glazes prepared with Ba-based frits but also for Ba-based glass ceramics and other frit-based glazes.

Acknowledgements The author would like to thank the Akcoat İleri Kimyasal Kaplama Malzemeleri San. ve Tic. A.Ş. and Seranit Ceramic Company for the materials and industrial conditions support.

Funding Open access funding provided by the Scientific and Technological Research Council of Türkiye (TÜBİTAK).

Declarations

Conflict of interest The author declares no competing interests.

Open Access This article is licensed under a Creative Commons Attribution 4.0 International License, which permits use, sharing, adaptation, distribution and reproduction in any medium or format, as long as you give appropriate credit to the original author(s) and the source, provide a link to the Creative Commons licence, and indicate if changes were made. The images or other third party material in this article are included in the article's Creative Commons licence, unless indicated otherwise in a credit line to the material. If material is not included in the article's Creative Commons licence and your intended use is not permitted by statutory regulation or exceeds the permitted use, you will need to obtain permission directly from the copyright holder. To view a copy of this licence, visit <http://creativecommons.org/licenses/by/4.0/>.

References

- Eppler, R.A., Eppler, D.R.: *Glazes and Glass Coatings*. The American Ceramic Society, Ohio (2000)
- Taylor, J.R., Bull, A.C.: *Ceramic Glaze Technology*. Pergamon, Oxford (1986)
- Casasola, R., Rincon, J.M., Romero, M.: Glass-ceramic glazes for ceramic tiles—a review. *J. Mater. Sci.* **47**, 553–582 (2012)
- Partyka, J., Lis, J.: The influence of the grain size distribution of raw materials on the selected surface properties of sanitary glazes. *Ceram. Int.* **37**, 1285–1292 (2011)
- Bou, E., Bordes, M.C., Felhu, C., Gazulla, M.F., Ferrer, F., Pasies, G.: Variables that determine the matt appearance of some ceramic floor and wall tile glazes. *Proceeding of VII world congress on ceramic tile quality Qualicer*, 349–364 (2002)
- Kronberg, T., Hupa, L.: The impact of wollastonite and dolomite on chemical durability of matte fast-fired raw glazes. *J. Eur. Ceram. Soc.* **40**, 3327–3337 (2020)
- Campa, F., Ginés, F., Robles, J.: Matting of a transparent porous wall tile glaze by adding alumina. *Proceeding of VI world congress on ceramic tile quality Qualicer*, 115–117 (2000)
- Sheikhhattar, M., Attar, H., Sharafi, S., Carty, W.M.: Influence of surface crystallinity on the surface roughness of different ceramic glazes. *Mater. Charact.* **118**, 570–574 (2016)
- Gorodylova, N., Dohnalova, Z., Kostal, P., Sulcova, P., Vlcek, M.: Impact of particle size reduction on glaze-melting behaviour, description by heating microscopy and Vogel-Fulcher-Tamman equation. *J. Therm. Anal. Calorim.* **116**, 605–612 (2013)
- Li, J., Liang, J., Wang, L., Wang, F.: Effect of particle-size distribution on the surface appearance of glazed surface. *J. Therm. Anal. Calorim.* **115**, 1127–1131 (2014)
- Wattanasiriwech, D., Wattanasiriwech, S.: Effects of particle size of glaze powder and thickness of glaze layer on glaze crawling for dolomite wares. *Chiang Mai J. Sci.* **33**(1), 35–44 (2006)
- Amoros, J.L., Blasco, E., Moreno, A., Marin, N., Feliu, C.: Effect of particle size distribution on the sinter-crystallisation kinetics of a $\text{SiO}_2\text{-Al}_2\text{O}_3\text{-CaO-MgO-SrO}$ glass-ceramic glaze. *J. Non-cryst. Solids.* **542**, 120–148 (2020)
- Amoros, J.L., Blasco, E., Feliu, C., Moreno, A.: Effect of particle size distribution on the evolution of porous, microstructural, and dimensional characteristics during sinter-crystallisation of a glass-ceramic glaze. *J. Non-cryst. Solids.* **572**, 121093 (2021)
- Felisbino, S.B., Milanez, K.W., Riella, H.G., Bernardin, A.M.: Influence of glaze particle size distribution on surface tension and gloss. *Proceeding of VIII world congress on ceramic tile quality Qualicer*, 201–208 (2004)
- Bernardin, A.M.: The influence of particle size distribution on the surface appearance of glazed tiles. *Dyes Pigm.* **80**, 121–124 (2009)
- Partyka, J., Lis, J.: Chemical corrosion of sanitary glazes of variable grain size composition in acid and basic aqueous solution media. *Ceram. Int.* **38**, 553–560 (2012)
- Taşkıran, F., Varışlı, S., Akkaşoğlu, U., Öztürk, B., Çiçek, B.: Investigation of the effect of glaze particle size distribution on surface properties of floor tile glazes. *J. Turkish Ceramic Soc.* **1**(3), 26–30 (2021)
- Burzacchini, B.: Use of the hot stage microscope to evaluate the characteristics and behaviour of frits and glazes at different heating rates. *Proceeding of IV world congress on ceramic tile quality Qualicer*, 701–709 (1996)
- Venturelli, C.: *Heating Microscopy and its applications*. Microscopy Today, (2011). <https://doi.org/10.1017/S1551929510001185>
- Jiang, Q., Zhang, S.H., Li, J.C.: Grain size-dependent diffusion activation energy in nanomaterials. *Solid State Commun.* **130**, 581–584 (2004)
- Santos, C., Koizumi, M.H., Daguano, J.K.M.F., Santos, F.A., Elias, C.N., Ramos, A.S.: Properties of Y-TZP/ Al_2O_3 ceramic nanocomposites obtained by high-energy ball milling. *Mater. Sci. Eng. A.* **502**, 6–12 (2009)
- Altındal, F., Anil, U.E., Varışlı, S.O., Öztürk, B.: Investigation of the effect of BaO- Al_2O_3 variations for BAS glass-ceramic glaze: Insights into thermal, phase, microstructural and surface features. *J. Eur. Ceram. Soc.* **44**, 3200–3209 (2024)

23. Silva, M.J.D., Bartolomé, J.F., De Aza, Mello-Castanho, A.H.: Glass ceramic sealants belonging to BAS ($\text{BaO}-\text{Al}_2\text{O}_3-\text{SiO}_2$) ternary system modified with B_2O_3 addition: A different approach to access the SOFC seal issue. *J. Eur. Ceram. Soc.* **36**, 631–644 (2016)
24. Melchiades, F.G., Rego, B.T., Higa, S.M., Alves, H.J., Boschi, A.O.: Factors affecting glaze transparency of ceramic tiles manufactured by the single firing technique. *J. Eur. Ceram. Soc.* **30**, 2443–2449 (2010)
25. Kingery, W., Bowen, H., Uhlmann, D.: *Introduction to Ceramics*. JohnWiley&Sons, New York (1976)
26. Santos, C.R., Fontana, T.L.B., Uggioni, E., Riella, H.G., Bernardin, A.M.: Achieving opacity in ceramic tiles: Microstructural and spectrophotometric analysis. *Proceeding of VIII world congress on ceramic tile quality Qualicer*, 189–194 (2004)

Publisher's Note Springer Nature remains neutral with regard to jurisdictional claims in published maps and institutional affiliations.